We are IntechOpen, the world's leading publisher of Open Access books Built by scientists, for scientists

6,900
Open access books available

186,000
International authors and editors

200M
Downloads

Our authors are among the

154
Countries delivered to

TOP 1%
most cited scientists

12.2%
Contributors from top 500 universities

CLARIVATE ANALYTICS
BOOK CITATION INDEX
INDEXED

WEB OF SCIENCE™

Selection of our books indexed in the Book Citation Index
in Web of Science™ Core Collection (BKCI)

Interested in publishing with us?
Contact book.department@intechopen.com

Applications of SR Drive Systems on Electric Vehicles

Wang Yan, Yin Tianming and Yin Haochun
Beijing Jiaotong University/Beijing Tongdahuaquan Ltd. Company/Tsinghua University
China

1. Introduction

As the continuous growth of global vehicle production and owned, the problems brought by vehicles are conspicuousness day after day. These problems are much more serious in China. Thus developing zero emission electric vehicles have become the main scientific research projects in many countries around the world in 21st century. Energy-saving motor drive technology has become one of the key points to the EV commercialization.

In the present electric vehicles, there are several main drive systems include the chopping system of DC motor, the variable frequency drive system of induction motor(IM), the drive system of permanent-magnet motor(PM) and switched reluctance drive system(SRM), etc. The DC machine has been faded gradually in the electric vehicle drive system for the reason of high startup current, huge volume, low efficiency and poor reliability. Even worse, the carbon body and the commutator which are not suited for high speed movement need to be changed frequently. The variable frequency drive system of IM has a small torque fluctuation, but with low efficiency especially in the low speed stage. When the electric vehicle is grade climbing, the torque output is small and the current is high. Although the permanent-magnet motor is of high efficiency, the manufacturing technique is very complicated and the machine will lose effectiveness because of the demagnetization in high temperature. So it is not the perfect way. The structure of the SR Motor is firmly and stable. The SRD system has a high reliability, wide range of speed regulation, high efficiency, low startup current and large torque output, all of which are especially suited for the work condition of the electric vehicles. The application of SRD on electric vehicles is affected by the torque fluctuation and strong noise. In a word, performance comparisons of the three motors are indicated in the following table 1.

Because of its own characteristics,electric vehicles motor drive system should meet the following demands:

1. Output a large torque under base speed to meet the requirement of starting, accelerating, climbing and some other complicated working conditions.
2. Output constant power above the base speed in order to adapt max speed, overtaking and so on.
3. Maximize motor efficiency over the whole speed range to extend endurance mileage.

From the table, the SRM has more advantage than the other motors.

Many control different strategies have been proposed for the torque fluctuation task . Full rotor pitched insulating non-magnetic colloid techniques of SRM and SRM fuzzy logic

adaptive torque control system based on instantaneous torque sum are proposed in this chapter.

Items \ Motors	IM	PM	SRM
System efficiency	lower	higher	higher
Starting torque	lower	higher	highest
Power density	lower	highest	higher
Workmanship	simple	complicated	simplest
Reliability	higher	lower	highest
Life	longer	short	longest
Manufacturing cost	lower	highest	lowest

Table 1. Performance comparisons of IM, PM and SRM

2. Design of SR motor on EV

The noise sources can be divided into four broad categories: magnetic, mechanical, aerodynamic and electronic . Therefore, according to the magnetic flux in the machine passing across the air gap in an approximate radial direction producing radial forces on the stator and rotor result in magnetic noise and vibrations, selection of 12/8 construction is used in the SRM design and a new rotor structure is proposed in this section.

2.1 Electric vehicle power demand

The selection of driving motor on electric vehicles mainly depends on rated power and rated speed. The more power grade is choosed the more reserve-power is got and the better vehicle driving feature is. But the volume and weight of the motor will increase rapidly by the same time and lead to the decline of the motor efficiency. So, the motor power should not too large. The calculation of power matching of EV motor is as follows:

A simplified model of the road vehicle dynamics can be used to estimate the tractive requirement of the vehicle drive-train, from which the individual component specifications can be rated with-regard-to their peak and continuous duties. The vehicle model accounts for the resultant forces acting against the vehicle when starting and when in motion, as illustrated in following figure 1. These forces can generally be considered as comprising of four main components, viz.:
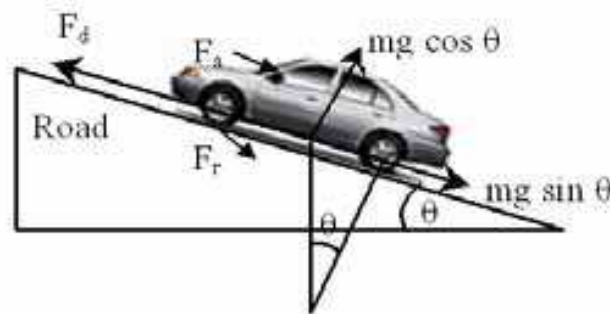
$$F_d = F_w + F_r + F_a + F_j \tag{1}$$

Fig. 1. Vehicles dynamics analysis

Where the force to overcome the tyre to road power loss, or rolling resistance, $Fr = kr \bullet mg \bullet \cos\theta$, a resistive force related to the road gradient, $F_w = mg \bullet \sin\theta$, an aerodynamic resistance or drag force, $Fa = 1/2 \bullet \rho C_d A_f v^2$, and the transient force required to accelerate or retard the vehicle, $F_j = m \bullet dv/dt$. Where:-
kr is the rolling resistance coefficient which includes tyre loss and is approximated to be independent of speed and proportional to the vehicle normal reaction force; m is the vehicle and payload mass; θ is the road gradient; g is the gravitational constant; ρ is the density of air; Cd is the drag force coefficient; A_f is the vehicle frontal area, and v is the vehicle linear velocity. Having determined the forces acting upon the vehicle, the road wheel torque can be calculated from the equation of motion, viz.:

$$T_w = J_w \cdot \frac{d\omega_w}{dt} + d_f r_w F_d \tag{2}$$

Where J_w, ω_w, r_w, are the wheel inertia, angular velocity and mean radius, respectively, and d_f is a factor proportioning torque distribution on the rear axle. By way of example, for a direct rear wheel drive scenario, it is assumed that there is an equal share of the required tractive force between each wheel drive machine (i.e. d_f = 0.5). For an on-board drive machine option, a gear stage is included in the drive-train, thus the output torque of the traction machine is related to the road wheel torque by the total transmission gear ratio, n_t, transmission efficiency, η_t, and the machine rotor inertia, J_m. Incorporating these into the equation of motion yields a general expression for traction machine torque:

$$T_m = J_m \cdot \frac{d\omega_m}{dt} + \frac{1}{n_t \eta_t} T_w \tag{3}$$

Expressing the wheel and traction machine angular velocities in terms of the vehicle linear velocity yields:

$$\omega_w = \frac{v}{r_w} \tag{4}$$

$$\omega_m = n_t \frac{v}{r_w} \tag{5}$$

From which the machine torque equation can be expressed in terms of the vehicle linear velocity by substituting eqns.(1), (2), (4) and (5) into eqn.3:

$$T_m = \left(\frac{n_t \cdot J_m}{r_w} + \frac{J_w}{n_t \eta_t r_w} + \frac{d_f r_w m}{n_t \eta_t} \right) \frac{dv}{dt} + \frac{d_f r_w}{n_t \eta_t} \left[\left(k_r \cos\theta + \sin\theta \right) mg + \frac{1}{2} \rho C_d A_f v^2 \right] \quad (6)$$

Mechanical power is torque multiplied by mechanical speed:

$$P_m = T_m \omega_m \quad (7)$$

Acording to the confirguration of the PEUGEOT 505 SW8 showed in table 2, the drive motor power can be calculated using above equations. $P_m = 26.36 kW$ .Considering batteries (weight 650 kg) will be added on the vehicle, the motor should be enlarged to 30kW.

the weight with full load	2000kg
rolling resistance coefficient	0.0267
air resistance coefficient	0.3
windward area	1.75m²
the average efficiency of motor	0.94
the density of air	1.205Kg/m³
the road gradient	15°
the max speed of EV	180km/h

Table 2. The parameters involved are listed in table 2.

Assume there are two motors with same rated power, the one with higher rated speed is smaller and lighter. In the view of vehicle performance, there will be less mechanical loss if the rated speed is higher. Meanwhile, it can provide large speed range to the drive system. Although the higher rated speed is favorable, the drive gear will be much more and more complicated. So, the above mentioned factors should be all considered in the selection of motor rated speed.

2.2 Designed SRM for PEUGOT 505 SW8

The parameters design of SR drive motor are contained the preliminary selection of frame size, the number of stator poles Ns and the number of rotor poles Nr, the stator and rotor pole angle selection, the bore diameter and the stack length, the selection of the conductor and the winding design, the calculation of the minimum and maximum inductance according to specifications for the SRM selected above, viz. 30kW, 4000r/min, 300v SRM. Then the motor verification is designed by Finite Element Analysis.

Following are the parameters of SR drive motor (Table.3), we choose 300V lead acid storage battery as power supply system. The mortor's performance curves are showed in figure 2, 3,4. The fig.2 gives the profile of flux linkage vs. current of unaliagned and aliagned stator and rotor tooth. The fig. 3 decribes when the rotor's angel changing, the stator's winding current changs. The fig.4 represents the composed torque of the motor changes with the angel. It shows big variety occurs commutation between the winding phase A and B or Band C et. Thus measurement should be taken to avoide the torque ripple.

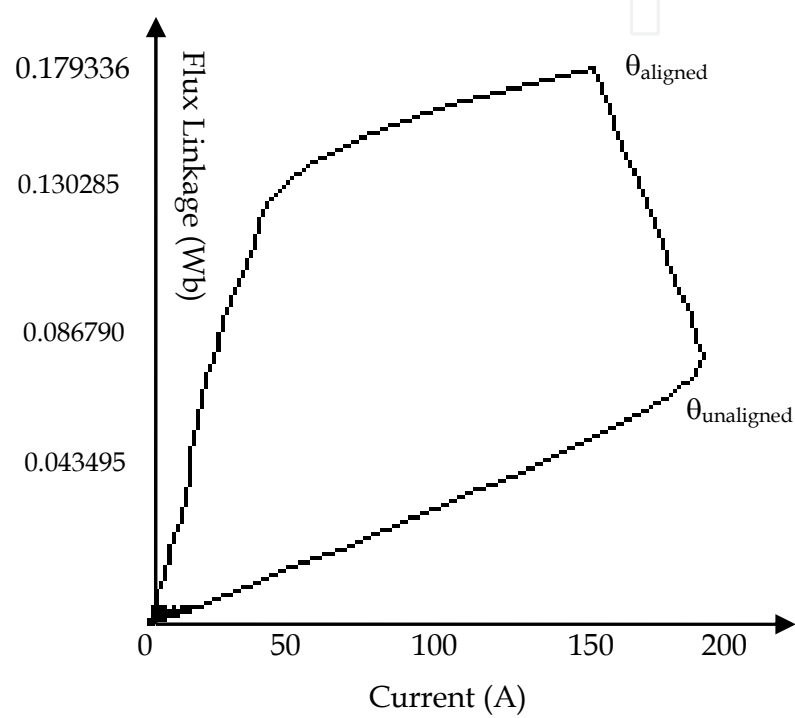| Rated power (kW)	30	Rated voltage (V)	300	Rated speed (r/min)	4000
Poles and phase	12/8, 3	Maximum value of phase inductance (mH)	3.98401	Minimum value of phase inductance (mH)	0.379135
Effective rated value of phase current(A)	88.6784	Motor average efficiency	0.94	Rotary inertia(kg*m²)	0.0486939

Table 3. The parameters of SR drive motor
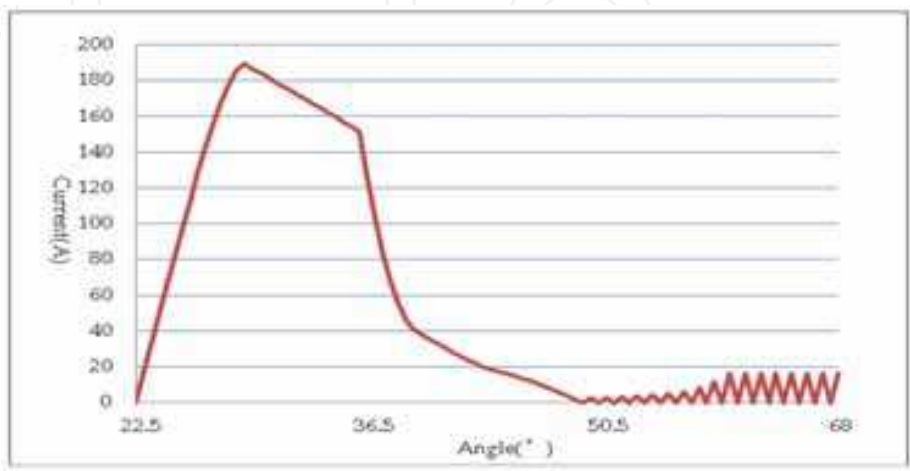

Fig. 2. Profile of designed SRM flux-linkage-current

Fig. 3. Profile of designed SRM current vs. angle
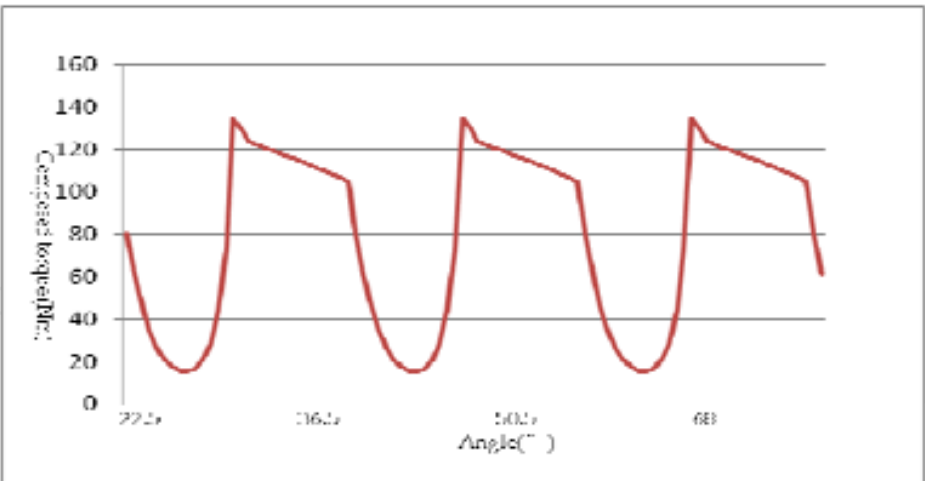
Fig. 4. Profile of designed SRM composed torque vs. angle

2.3 New rotor structure

There are large spaces between the present SRM rotor teeth, which will cause strong noise when the rotor rotating. A new type of rotor structure is proposed in the chapter. Figure 5 (a) shows the originally one, (b) (c) is the new structure diagrammatic sketch.The structure include 1 shaft, 2 rotor tooth, 3 yoke part, 4 screw bolt and nut, 5 insulating non-magnetic colloid, 6 copper collar, 7 steel ring. The insulating non-magnetic colloid is filled in the yoke part between rotor teeth. The two copper collars which are used to fix insulating non-magnetic colloid by screw bolt and nut are connected through the rotor shaft.

The expansion factor of insulating non-magnetic colloid is similar to rotor silicon-steel sheet, which can avoid the fissure between insulating non-magnetic colloid and rotor teeth. There are small amount of heat and noise when the new SRM rotor structure is applied during high speed rotating. It is obvious that the working efficiency is higher than the existing one.
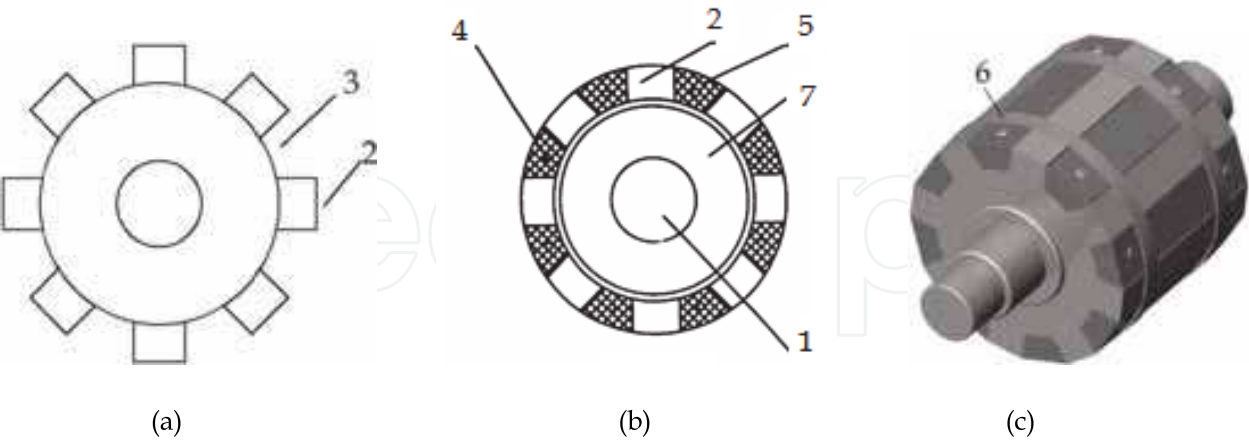

| (a) | (b) | (c) |

Fig. 5. A novel rotor structure for SRM

2.4 Drive mode for PEUGEOT 505 SW8

At beginning development of electric vehicles, inorder to concentrate to develope battery cell and drive motor system, electric vehicles conversion design is usually adopted. The most defferent between the electric and regular fuel vehicles is energy system. Dynamic

system of the EV is composed of battery system and drive motor system. The battery provides direct current supply. The supply passing through electric apparatus which is made of controller and power main electical circuit is changed into electical power which can be used by the motor. Then the motor runs and the wheels are drived. The energy power transmission is showed in following figure 6.

The PEUGEOT 505 SW8 is a kind of wagon which is drived by rear-wheel. So the conversion EV can be designed as the motor connecting to gear-box via clutch, transaxle driving the wheels through transmission shaft. The drive mode is shown in figure 7.
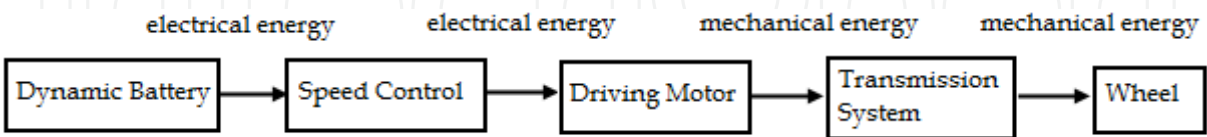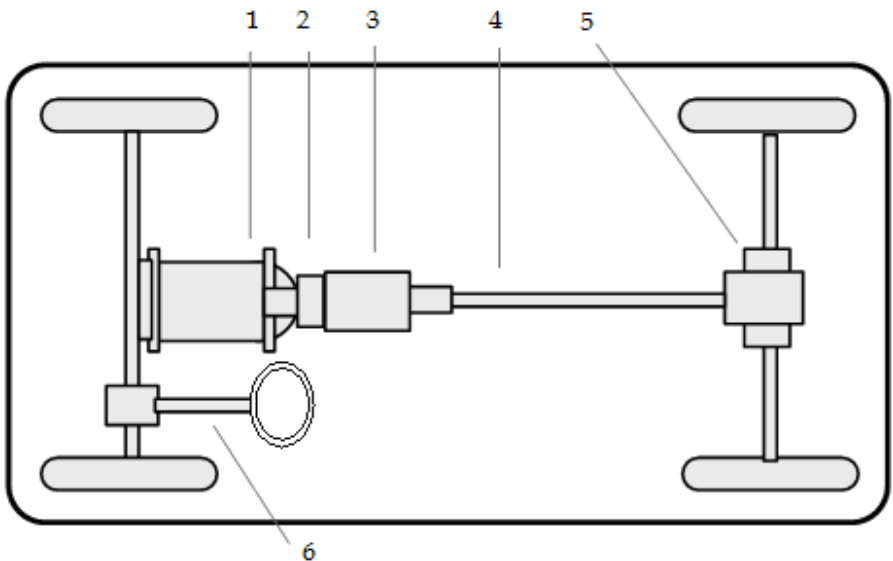

Fig. 6. The power transport process of EV

1- motor, 2-clutch, 3-gear-box, 4-transmission shaft, 5-transaxle, 6-steering gear

Fig. 7. Drive mode for PEUGEOT 505 SW8 conversion

3. SR drives power converter

The cost and performance of the SRM drive have been determined by many or converter topologies invented, and unlike the conventional inverts-fed induction machine, the SRM drives are highly dependent on the convert topology used to dive the SRM. An asymmetric half bridge converter topology is adopted in the 3-Phase SRM drive for EV, which is showed in figure 8. The main electrical circuit composes of power electrical lead acid batteries U_s, support capacitor C_s, asymmetric half bridge IGBTs from V11 to V62 and freewheel diodes from VD11 to VD62. It permits control of the individual phases fully independent of each other and thus permits the widest freedom of control. During normal operation, the electromagnetic flux in an SR motor is not constant and must be built for every stroke. In the motoring period, these strokes correspond to the rotor position when the rotor poles are approaching the corresponding stator pole of the excited phase. In the case of Phase A,

shown in figure 8, the stroke can be established by activating the switches V11 and V42. At low-speed operation the Pulse Width Modulation (PWM), applied to the corresponding switches, modulates the voltage level. When the switches V11 and V42 are turned off in the same time, producing transformer electromotive force in Phase A break-over forward freewheel diodes VD11 and VD42, the Phase A current after flows through VD11, VD42 and Cs. Each of V11 with its anti-parallel diode VD11 and V12 with its anti-parallel diode VD12 is the asymmetric half bridge structure in the one IGBT module. KDC is a DC contactor which powers up to the drive system, and is controlled by key of the vehicle which starts the engine originally.
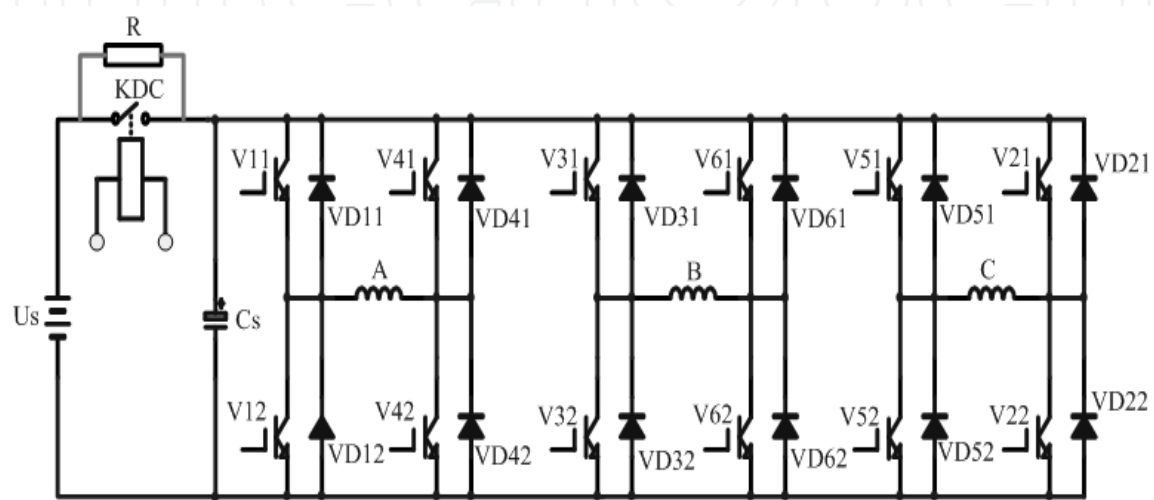

Fig. 8. Schematic Diagram of Power converter in Electrical Vehicle

3.1 Parameter selection of the main circuit

The driving power U_s is composed of 25 series lead acid batteries which rated voltage is 12V, capacity is 85Ah. Thus the whole volume of U_s is 300V. Because safety working voltage arrange of the single battery is from 10.5V to 14.4V, the actual group of batteries working voltage arrange is from 262.5V to 360V. Selecting maximum DC bus voltage 360V, in the asymmetric half bridge main circuit the main switch IGBT will bear the maximum DC power voltage from the bus. Considering twice surplus capacity, the IGBT withdraw voltage is in equation 8.

$$U_r = 2U_{smax} = 2 \times 360V = 720V \tag{8}$$

The effective rated value of the phase current for the designed SRM is 88.6784A, considering the overloade current of the drive system two multiple of the phase current, the effective rated value of the IGBT current is in equation (9).

$$I_{srms} = 2I_N = 2 \times 88.6784A = 177.3568A \tag{9}$$

Having determined the effective rated value of the IGBT current , the peak current of the IGBT can be calculated in equation (10), viz

$$\hat{I}_S = \sqrt{2} \times 2 \times \sqrt{q} I_N = 434.3553A \tag{10}$$

In the equation (9), *m* is the number of the phase of the SRM which eaquals 3 in the system. Actually power converter parameters involved in the designed SR drive motor are listed in table 4. To sum up , the main circuit switch IGBT can be selected as BSM300GA120DLC of EUPEC which has 1200V bear voltage ($T_C = 80^0 C$), 300A effective current value, 600A peak current value ($t_p = 1ms$).

Electrical parameters	Values
Average current of main switch	46.1426 A
Effective current of main switch	84.7971A
Peak current of main switch	188 A
Average current of after flow bidiode	11.878A
Effective current of after flow bidiode	27.0406 A
Peak current of after flow bidiode	138A

Table 4. Designed Parameters of SR Drive Motor

3.2 IGBT drive and snubbed electronic circuits design
IGBT is simply voltage driven switches, because their insulated gate behaves like a capacitor. Conversely, switches such as triacs, thyristors and bipolar transistors are "current" controlled, in the same way as a PN diode. Because IGBT gate drive condition is closely related to its static and dynamic performance. The turn-on voltage, switching time, switching loss, short-circuit withstand capability etc. are ordinately effected by positive and negative voltage (V_{GE} and - V_{GE}) between gate and emitter, gate electrode resistance (R_G). Being reasonably designed drive and protection circuit is quite important.

3.2.1 IGBT drive conditions
The concrete requirement of IGBT drive circuit is listed flowering.
(1)Because IGBT is a type of voltage drive module, it has a threshold voltage value of 2.5 V to 5.0V and has a capacitive input resistance. IGBT is very subtle to electric charge accumulation of the gate electrode, so the drive circuit must be very reliable to grantee there is a discharge loop with a low resistance itself, viz. there is as short as possible wire between the circuit and IGBT.
(2)Charging and discharging the gate oxide capacity with small interresistance drive supply inorder to gurantee that the gate electrode controlling voltage has much enough steep forward and reverse edge. Because IGBT has nonlinear capacitive character, the driver must have enough instantaneous absorbing current capability. Thus the gate electrode voltage can be set up or disappear soon inorder to decrease the switch loss lowerly. On the other hand, after the IGBT turns on, the gate electrode driver should supply enough power to avoide to be destroyed because of exit saturation. The drive interresistance can not be lower than commanded R_G, otherwise there will have underdamped harmonic motion between the stray inductance and the gate electrode capacity in the drive loop . Meanwhile, the surge current increases during short switching time. This induces booth unsafty in the main circuit and disturbance in the control circuit.
(3)Although the higher + V_{GE}, the higher current limit becomes, + V_{GE} should be remained under maximum rated G-E voltage, + V_{GES} =+20V. The reason is once there is a over current

or short current, the higher + V_{GE}, the higher current, the bigger probability of the IGBT destroy becaues the time of enduring short current capability decreases. Usually, the value of + V_{GE} is considered as between 12V and 15V.

(4)Set the enough gate reverse bias voltage value(-V_{GE}) to IGBT. While the IGBT is in off-state, there are some high frenquency osillation signals in the gate electrode circuit because the other part circuits are stiill working. These signals may let IGBT to be in micro on-state, it results in the power loss of IGBT increase.   Therefore a recommended -V_{GE} to IGBT is -5V to -10V (the maximum gate reverse bias voltage value is -V_{GES} =-20V), so that the IGBT can be cut off reliably even if there are switch noises in the gate electrode of IGBT .

(5) The gate electrode resistance effects R_G on the switch loss, switch speed, and even involves in whether the drive circuit appears oscillation and the collector electrode generates surge current. Usually the value of R_G can not be selected to be over 10 times than the producer recommended value. In actual application, R_G should be ajusted carefully. R_G should be disposed closely to the gate electrode.

(6) There should be have a gate electrode amplitude limiting circuit to avoid to breakthrough the gate electrode.

(7) The drive circuit should be isolated from the control circuit so that, when the IGBT is destroyed the other components can not be damaged. When the IGBT burns, the collector electrode high voltage usually pwties the drive circuit through destroyed the gate electrode, and then disrupts some components in the drive circuit . The gate electode drive circuit as far as possible should be simple and actual. It is much better that the IGBT itself has protection and very strong the ability of disturbance. When the IGBT is under the state of load short circuit or over current, the IGBT can prevent fault current automatically through decreasing the gate electrode voltage gradually to be switched the IGBT off softly. That is to prevent very high di/dt causing by the fault current because of IGBT turn-off swiftly . The high value di/dt can produce high spiking voltage under the stray inductance function, results in the IGBT to be unbearable and damaged. By the same rule, the soft turn-off process of the drive circuit should not be effected by the input signal disappear. The drive circuit should have a time logical for thegate voltage control function. When there has over current, no matter whether there is the input signal, the drive circuit should be turned off unconditionally.

3.2.2 IGBT drive electrinic circuits design

The IGBT-driving hydrid IC EXB841 produced by Fuji Electric is used in the EV power convter. It can drive 300A/1200V or 400A/600V IGBT moduel and the drive signal delay reaches 1.5μs, the maximum switching speed is 40KHz. The drive circuit is designed in figure 9 arround EXB841, in which C1 and C2 are two electrolytic capacitors to absorb the chang of supply voltage. MC1413,LED,R1,R2 are composed of the drive line from the control circuit to EXB841. V3 and V4 are two voltage-stabilizing diodes to limit amplitude of EXB841 output drive voltage, so that to avoide the drive voltage higher and destroy the IGBT. V3 and V4 are two voltage-stabilizing diodes which are in inverted series and connected in parallel with collector and emitter electrode. The over current protective circuit for IGBT is composed of R3, E1,R4, V1 and V2, in which V1 and V2 connecting to the sixth pin of EXB841 completes to monitor the collector electrode voltage. V1 is the fast recover diode which is ERA 34-10 made from Fuji Electric. V2 is the voltage-stabilizing

diode which can change the controlled point of the current protection by adjusting the voltage-stabilizing value of the diode. Theoretically, if the over current protection of EXB841 takes effect is that the pin of EXB841 outputs a low electrical level when the collector electrode voltage monitoring the six pin is greater than 7.5V. Then the opto-coupler in the figure outputs a fault signal to the control board which is high level OC signal. The signal produces interruption on the board and controls CPU to block trigger pulse for IGBT. The theoretical protective value 7.5V of EXB841 is the operating point which the supply voltage is strictlly controlled at 20V. When the supply voltage has ripple or error, the protective value will change. When the supply voltage is greater than 20V, the protective value increases 1V as the supply voltage does. When the supply voltage of EXB841 is 20V, the drive voltage suppllied IGBT turning on is 15V. According to the profile of switching losses of IGBT-inverter of BSM300GA120DLC, the curve of collector electrode current vs. IGBT switching on voltage drop V_{CE} can be abttain. The voltage drop between the gate and the emitter electrode can be calculated in the following equation and figure 10.
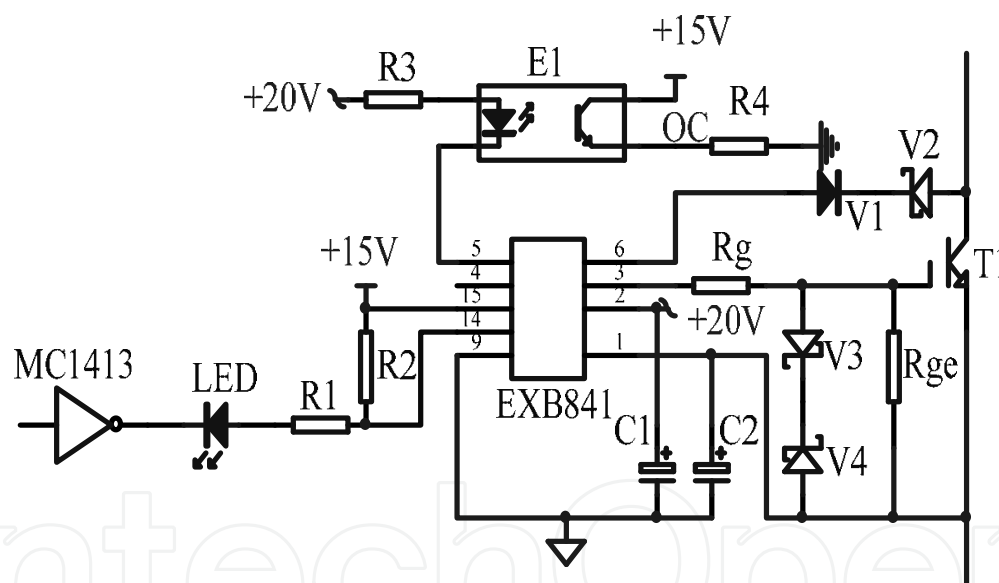
$$V_{CE} = RI_C + V_0 \tag{11}$$

Fig. 9. IGBT drive circuit

According to the figure 10 and 11, when $T_{vj} = 125°C$, IGBT output curve can be linearized by line $y=Ax+B$. Known the three points on the curve, respectively they are (2.0,208), (2.5,325), (3.0,465). Using the points (2.0,208) and (2.5,325), the equation is listed in 12.

$$V_{CE} = 0.0042735I_C + 1.01282 \tag{12}$$

Taking $I_C = 480A$, $V_{CE} = 3.0641V$, the error of V_{CE} and the percent rate of error are listed in following equations.

$$\Delta V_{CE} = 3.0641 - 3.06 = 0.0041 \tag{13}$$

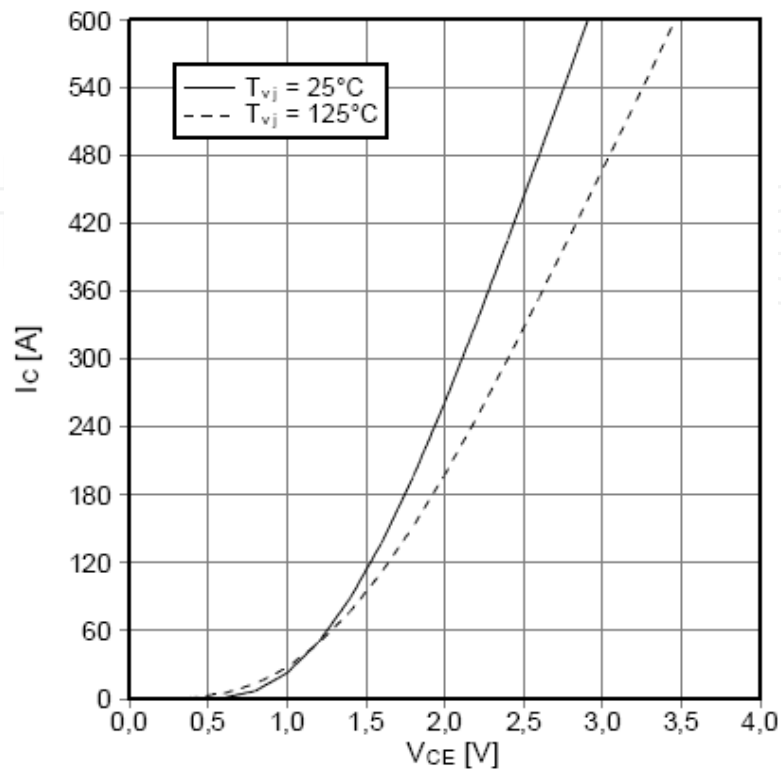$$\eta = \frac{0.0041}{3.06} \times 100\% = 0.133\%\qquad(14)$$

Fig. 10. IGBT BSM300GA120DLC output curve under different voltage

When the drive voltage suppllied IGBT turning on is 15V, the collector electrode current is 600A, IGBT switching on voltage drop V_{CE} is about 3.5V calculated by 12 and in figure 10. Then the value of voltage-stabilizing diode V2 is selected as 9V. From the table 5, the gate resistance value can be chossed 3.3Ω.
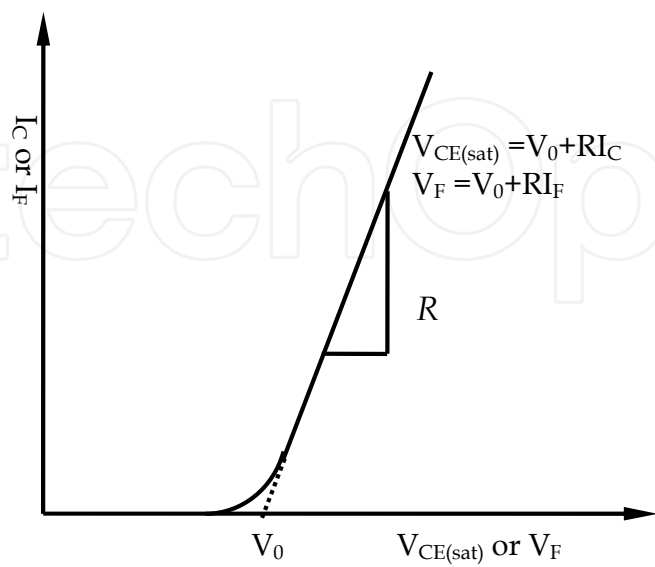

Fig. 11. Positive output characteristic curve of power devices

IGBT Rating	600V	200A	300A	400A	-
	1200V	200A	150A	200A	300A
R_G		12Ω	8.2Ω	5Ω	3.3Ω
Icc	5kHz	20mA	22 mA	23 mA	27 mA
	10kHz	24 mA	27 mA	30 mA	37 mA
	15kHz	27mA	32 mA	37 mA	47 mA

Table 5. Recommended the gate resistance R_G and the current loss

3.2.3 IGBT snubbed electronic circuits design

When the power electronic device is used, buffer electronic circuit should be designed to inhibit respectively *di/dt* and *dv/dt* when the device switched on and off. The aim is to change switch locus of the device in order to avoid the maximum value of V_{CE} and i_C appear at same time. Thus the switching loss is decreased and reliability can be improved. T he IGBT snubbed electronic circuit is put particular emphasis on the voltage absorbing and restraining in switch on state. That is because the IGBT working switch frequency is very high, tiny inductance in the electronic circuit can cause very big *L di/dt* and produce over voltage to endanger the IGBT security. RCD snubbed electronic circuit is often used which is designed in figure 12. The RCD bridges joint every IGBT module connecting with two ends of the power. Capacity and resistance value selection has much more relationship with snubbing voltage in the snubbed electronic circuit. If the selection is improper, it would affect the voltage absorb so far as to bring about osillation in the circuit.

Within the IGBT switching off process, the current of device drops fastly, the current in the snubbed circuit increases at same change rating. The magnetic energy stored in the parasitic inductance in the main electronic circuit will wholly transfere into the electrical energy in the absorbing capacity. Assuming the current flowing the main switch device drops linearly when switching off, the current flowing the snubbed circuit increases linearly because the switching off process is very short. These two current can be expressed in the following equations.

$$i_T = (1 - \frac{t}{t_f})I \tag{15}$$

$$i_C = I - i_T = \frac{t}{t_f}I \tag{16}$$

In the equations, i_T is the current in the main switch device; i_C is the charging current in the absorbing capacity; t_f is dropping time when switching off. I is the average current in the direct current bus line. Therefore, the voltage of capacity two ends is expressed in the equation 17.

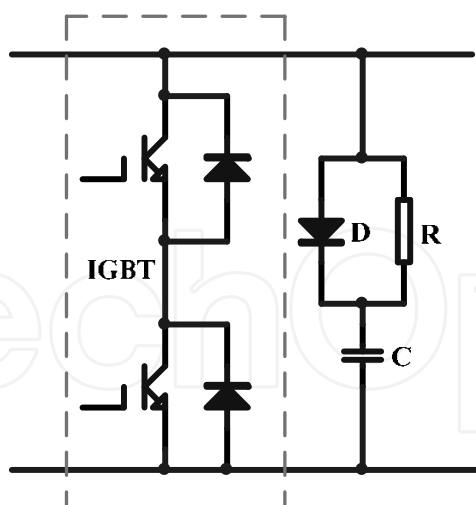$$U_{CS} = \frac{1}{C}\int_0^{t_f} i_C dt = \frac{1}{C}\int_0^{t_f} \frac{t}{t_f} I dt = \frac{It_f}{2C} \tag{17}$$

Fig. 12. IGBT snubbed elctronic circuit.

The capacity voltage U_{CS} usually can be selected as 10 to 50 percent of the supply voltage U_{DC} at t_f. For example, selecting $U_{CS} = 0.5U_{DC}$, the capacity C is in the following equation.

$$C \geq \frac{It_f}{U_{DC}} \tag{18}$$

The value of the absorbing capacity can be selected as 0.47μF according to the the equation 18 and experience value. The selection rule of resistance R is to releasing electric charge thouroghly stored in the snubbed capacity before the IGBT switching off signal comes. If R is too large, it makes the discharging time of the capacity C lower. But if R is too small, the discharging current is too large and fast when the IGBT switching on, it can endanger the device security and cause the osillation. So period (T) of the switch device eaquals 1 or 2 times of $3RC$. So the value of the resistance R can be calculated in the equation 19.

$$R \leq \frac{1}{6 \times C \times f} \tag{19}$$

R calculated by the equation 19 can not be greater than 41.72 ohm , 39ohm is selcted in the RCD snubbed circuit. The maximum power loss on the absorbing resistance can be calcultaed as in the equation 20.

$$P_R = \frac{1}{2}C\Delta V^2 f = 20W \tag{20}$$

The fast recovery diode is selected as FR607. Beside the IGBT drive and snubbed electronic circuits design, the switched power supply circuit and control circuit should be designed. Because the length of the chapter, the content cannot be covered all the bases. As figure 13 shows, the control circuit structure of SRD system is given. With MICM2002 (Motor Intelligent Module) based on DSP and AT89C51 singlechip the folowing control strategy is realized. When the EV is powered, the controller goes into working state. The control signal from all kinds of fault signals and the driver operating system are coded and loaded the

AT89C51 through prior coder. If the system is checked with no fault and no operation, the system is in standby mode. When the driver gives the start and throttle given signal, according to the SRM rotor position signal from the position sensor, the singlechip sends out the phase turn on/off signal and the MCIM produces the PWM signal, then the system integrates the protective and the current chopping signals to give the main circuit IGBT drive signal and control the power main circuit to supply the SRM windings electricity and move the motor. According to the positive and negative rotation setting and the position information of the motor, the singlechip controls the windings power-on sequences. When the motor rotates at low speed, current chopping control mode can be used. Firstly, the chip gives the upper limitation of the current chopping signal and puts it into the MICM through D/A converter; secondly, the MICM comparates the current limitation with the phase current detecting from the current sensor, then calculates, optimizes and sends out the chopping signal. When the motor speed arrives above basic speed, the control mode changes into angle control from the current chopping control. When the driver changes the operting signal, the control circuit changes the working logic and implements corresponding dive requirement through the power circuit. If there is fault in the motor running, the control circuit blocks the trigger pulse of IGBT and protects IGBT, and displays and alarms through display circuit. Meanwhile it communiates with CAN module and sends the fault signal to driver video facility.
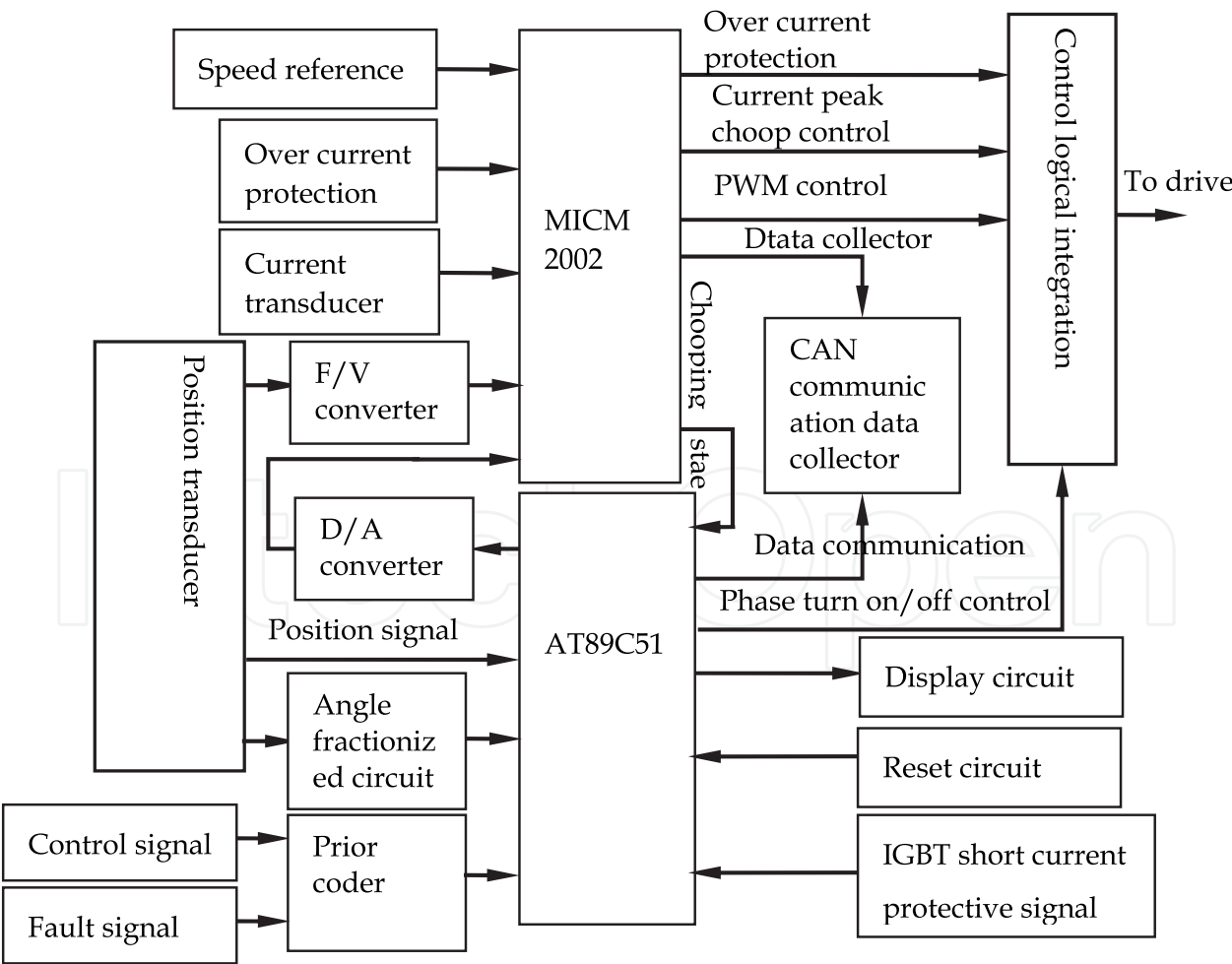

Fig. 13. Control circuit structure of SRD systems

4. SRM fuzzy logic adaptive torque control system

For the reason of the non-linearity in magnetic circuit, the SRM is hard to analyze and control. Also, it is difficult to build an accurate mathematical model. The fuzzy control are mainly applied to the system which is severely non-linearity or hard to get the mathematical model. The fuzzy adapative control to the SRD system is proposed in order to further increase the speed regulating precision and minimize the torque fluctuation. This chapter presents a new type of SRM control system which combines the PI regulator and fuzzy logic control－the SRM fuzzy logic adaptive torque control system based on instantaneous torque sum.

4.1 Speed PI regulator design

Figure 14 presents the principal frame of SRM fuzzy logic adaptive control. The conventional PI regulator is applied in the external loop and the fuzzy logic adaptive control based on instantaneous torque sum is used in the inner loop system. According to the voltage balance equation of SR motor:

$$V_i = R_s i_a + \frac{d}{dt}(La i_a) = R_s i_a + La\frac{di_a}{dt} + i_a\frac{dLa}{dt} = R_s i_a +$$
$$La\frac{di_a}{dt} + i_a\frac{dLa}{d\theta} \bullet \frac{d\theta}{dt} = R_s i_a + La\frac{di_a}{dt} + i_a\omega \bullet \frac{dLa}{d\theta} \tag{21}$$

Suppose the inductance change rate is constant, which defined as g_L .

$$g_L = \frac{dL_a}{d\theta} \tag{22}$$

So the equation 21 can be written as following equation.

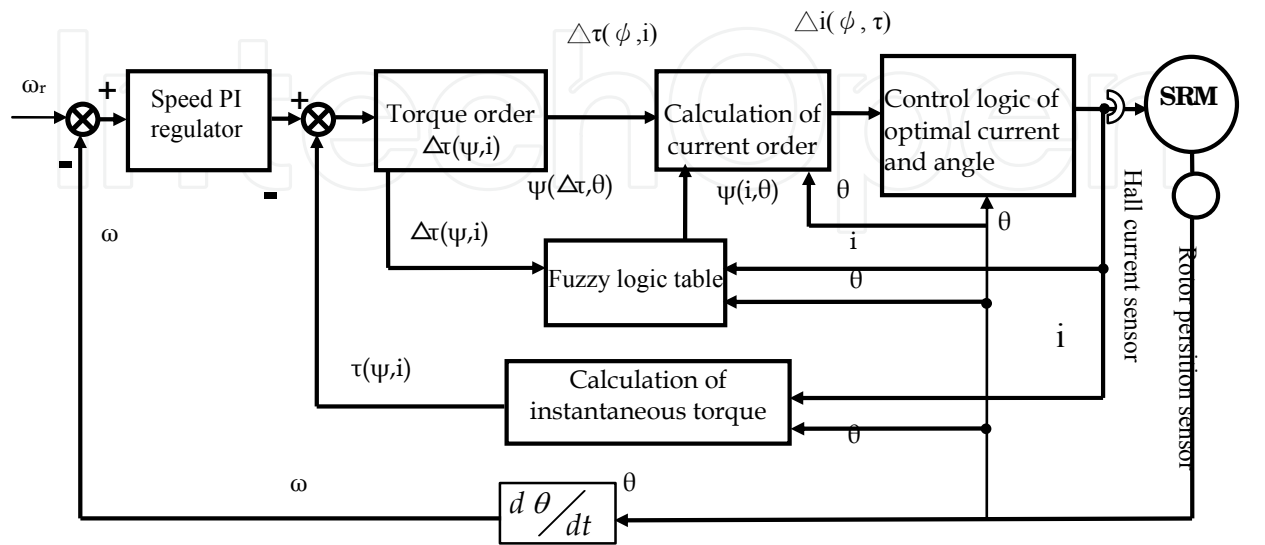$$V_i = (R_s + \omega g_L)i_a + La\frac{di_a}{dt} \tag{23}$$

Fig. 14. Principal frame of SRM fuzzy logic adaptive direct torque control system

The electromagnetic torque created by phase A is:

$$\tau_e(\theta,i) = \frac{1}{2} g_L i_a^2 \tag{24}$$

According to the torque balance equation 25:

$$\tau_e(\theta,i) = \sum_{n=1}^{3} \tau_{dn} = \tau_L(\omega) + k_\omega \omega + J\frac{d\omega}{dt} \tag{25}$$

When the system enters steady state, the torque is invariable:

$$\tau_e(\theta,i) = \sum_{n=1}^{3} \tau_{dn} = \tau_L(\omega) + k_\omega \omega \tag{26}$$

$\tau_L(\omega)$ is load torque and k_ω is coulomb friction coefficient.
Compare equation (7) with equation (8), we get:

$$\Delta\tau_e(\theta,i) = J\frac{d\omega}{dt} \tag{27}$$

If the sample time T is small enough, load torque and $k_\omega \omega$ can be seen as constant in the sample interval. So $\Delta\tau_e$ (ω) is proportational to $\Delta\omega$, equation (28) is:

$$\Delta\tau_e(\theta,i) \approx J \bullet \frac{\Delta\omega}{T} \tag{28}$$

In the equation above, $\frac{d\omega}{dt} \approx \frac{\Delta\omega}{T}$. Thus we get the torque deviation signal from speed deviation signal through the PI regulator.

$$\Delta\tau_e(\theta,i) \approx K_p \bullet \Delta\omega \tag{29}$$

The bandwidth of speed closed loop is small. It will be better when the proportional regulator used. But it is hard diminish to the steady-state error. So, in order to minimize the steady-state error and strengthen the disturbance rejection ability, we select the PI regulator. Equation 30:

$$\Delta\tau_e(\theta,i) \approx \left(K_p + \frac{K_i}{s}\right) \bullet \Delta\omega \tag{30}$$

4.2 Fuzzy controller design

From the figure 14, the inner loop is a direct torque control loop which is a three dimension self-adjust fuzzy logic control system, in which the torque loop is composed of the instantaneous sum torque negative feedback control. The inner loop is completed by software to complish the feedback of the fuzzy logic control itself, so that the SRM can be controlled in an optimal state. The following detail is about the fuzzy logic controller design and the adaptive "soft feedback" complement.

4.2.1 $\{(\theta,i) \to \psi\}$ **Fuzzy logic tables**

The SRM is multi input multi output controlled object. The fuzzy logic table describes the connection between input and output. In mathematics, this table can be seen as a two input single output non linear functions. The steps to build the table are as follows:

First step: confirm input and output fuzzy domain and its membership function.

Input variable is the rotor position angle and winding current. Their corresponding variation range are $0-45^0$ and $0-200A$. In order to improve learning rate, we assign that the membership function of fuzzy system input is isosceles triangle and its vertexes are located in the centre of triangle bottom. Shown in figure15(a)(b). The membership function of output flux linkage is shown in figure15(c) and its corresponding range is 0-0.18Wb. The fuzzy subset of linguistic value which describes input and output value are: $\{S,M,B\}$, which S=Small,M=Medium,B=Big.

$$R_i : if \quad \theta \quad is \quad A_i^{M\theta(n)}, \quad i \quad is \quad B_i^{Mi(n)} then \quad \psi \quad is \quad C_i^{M\psi(n)} \tag{31}$$

Second step: generate fuzzy rules from input data.

When every membership functions of input and output fuzzy domain is confirmed, we can get fuzzy rules from the measured data. Every input-output data pair is consist of current, rotor position and flux linkage which has specifically numerical relationship. In the first place, we get the membership degree from the corresponding fuzzy membership domain. Second, we assign the max membership degree to the variable in the domain. So, the value of nth data pair is $\theta(n)$, $i(n)$, $\psi(n)$. The assigned value will point to the fuzzy domain with the max membership degree, which can be written as the following fuzzy rules. In this equation, $A_i^{M\theta(n)}, B_i^{Mi(n)}, C_i^{M\psi(n)}$ are respectively represent the fuzzy domain of discrete data to $\theta(n)$, $i(n)$, $\psi(n)$. Table 2 is fuzzy rules. For example, if current is max and rotor position is max, the flux will be max.

Third step: confirm fuzzy rules membership degree.

When every new fuzzy rule is created from the input output data pair, a rule degree or fact is connected to this rule. The rule is defined as trust degree to the fuzzy rule. Actually the rule degree is related to the function, which describes the relationship between current, angle and flux linkage. The rule degree equals to the product of membership degree in each fuzzy domain. Like equation 31, can be depict as equation 32.

$$Degree(Rule) = \mu_{A_i^{M\theta(n)}} \times \mu_{B_i^{Mi(n)}} \times \mu_{C_i^{M\psi(n)}} \tag{32}$$

The instantaneous torque sum can be get from current, the rotor position angle and flux linkage in the following fuzzy logic table (Table 6).

4.2.2 Fuzzy model trainning

The phase current *I* is obtained by magnetic balance Hall current sensor and the angle *θ* by photoelectric position sensor. The flux linkage is calculated by the finite element analysis of current and the rotor position angle. The torque order is acquired from rotate speed order and then the current order is get from the torque order. Thus the current control can be realized. Figure 16 is the fuzzy controller based on MATLAB fuzzy toolbox. Figure 17 shows

the finite element analysis $\psi - i - \theta$ graph. According to finite element data, the model is training in the offered Matlab fuzzy toolbox. Figure 18 presents the $\psi - i - \theta$ graph acquired by training the static data in fuzzy model. As we can see from the Figure 17, the established fuzzy rules are correct that we can get accurate flux linkage ψ from the input phase current and the rotor position.
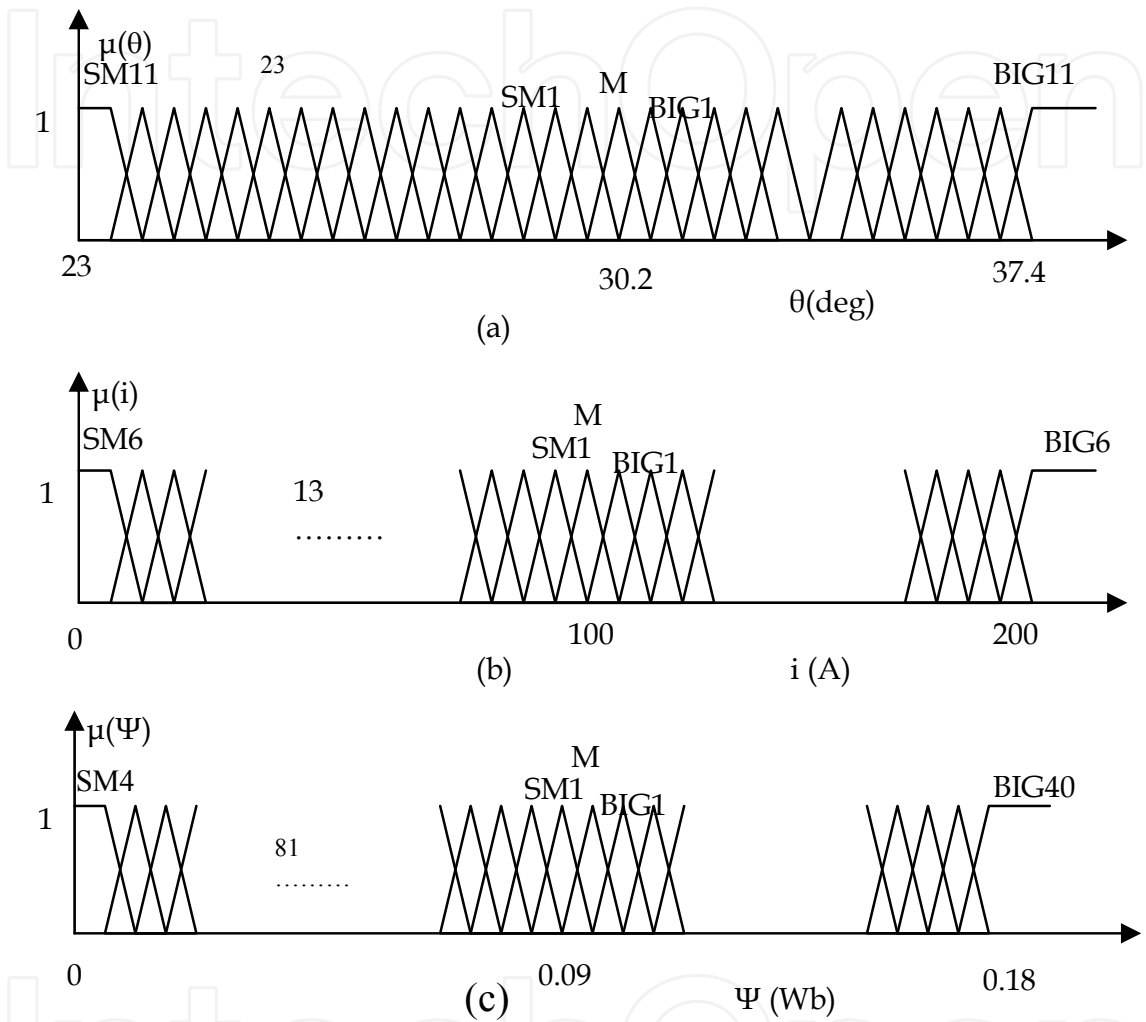

Fig. 15. Fuzzy domain regions and membership for each variable (a) Rotor position, (b) Current, (c) Flux linkage

		Flux linkage		
	Medium (M)	S	M	B
	Big (B)	S	S	B
Current		Small (S)	Medium (M)	Big (B)
		Rotor position		

Table 6. Fuzzy logic table between ψ and $i - \theta$

5. Result

5.1 Tests on the motor platform

Before the experiment on vehicle, we do the bench load test with the selected motor first. The experiment table includes three phase dynamometer, torque measurement oscilloscope, DC generator, resistance box and so on. The DC power needed by EV drive is supplied by 25 lead acid traction batteries. DC generator and resistance box make up the load of the
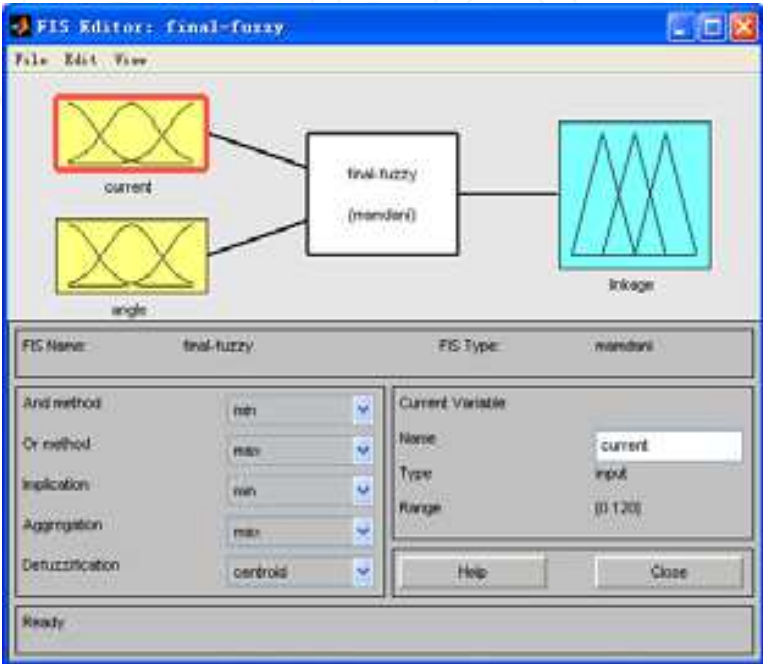

Fig. 16. Variation of the flux linkages of FEM for a single phase winding with rotor position and phase current
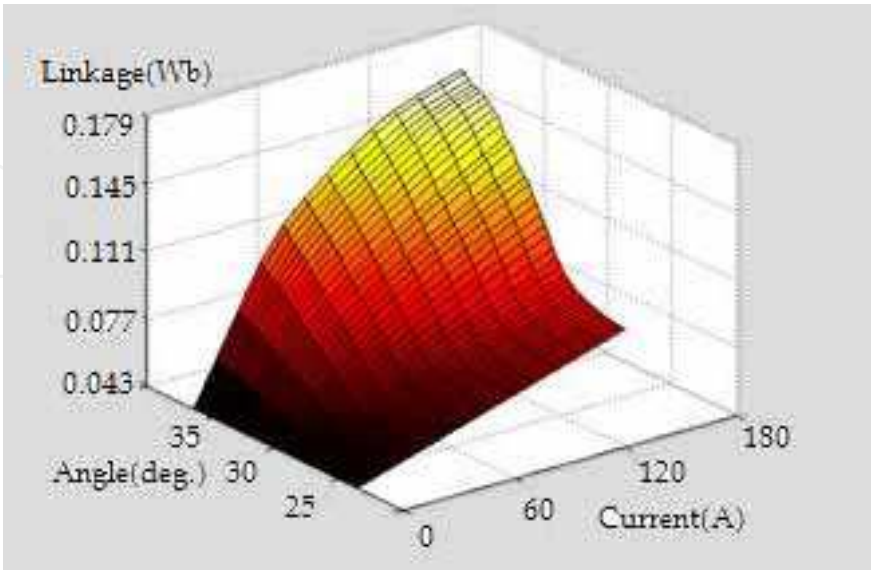
Fig. 17. Variation of the flux linkages of FEM for a single phase winding with rotor position and phase current
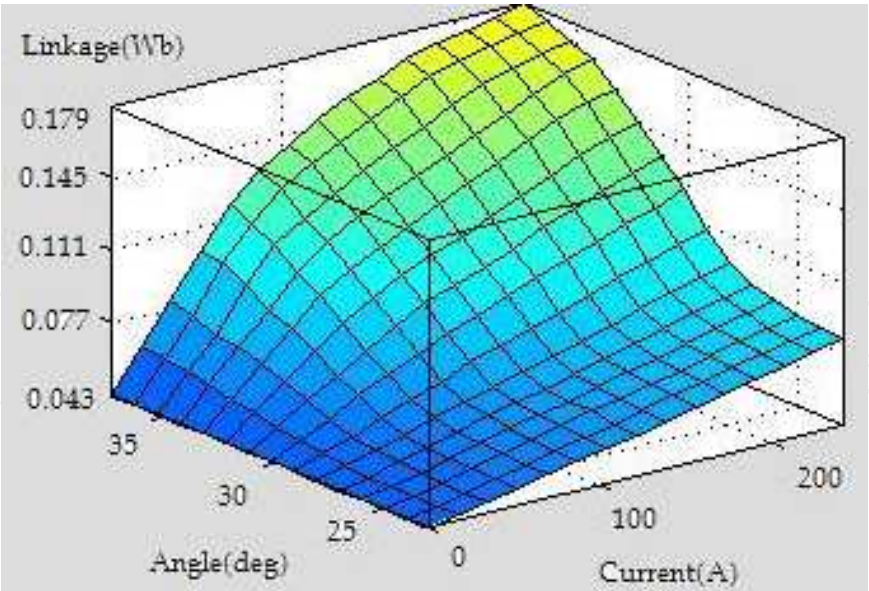
Fig. 18. Variation of the flux linkages of fuzzy controller for a single phase winding with rotor position and phase current

drive motor, which is adjusted by excitation voltage.Figure 19 shows the two phase winding current waveform of SRM when the motor speed at 500r/min and load with rated torque. From this figure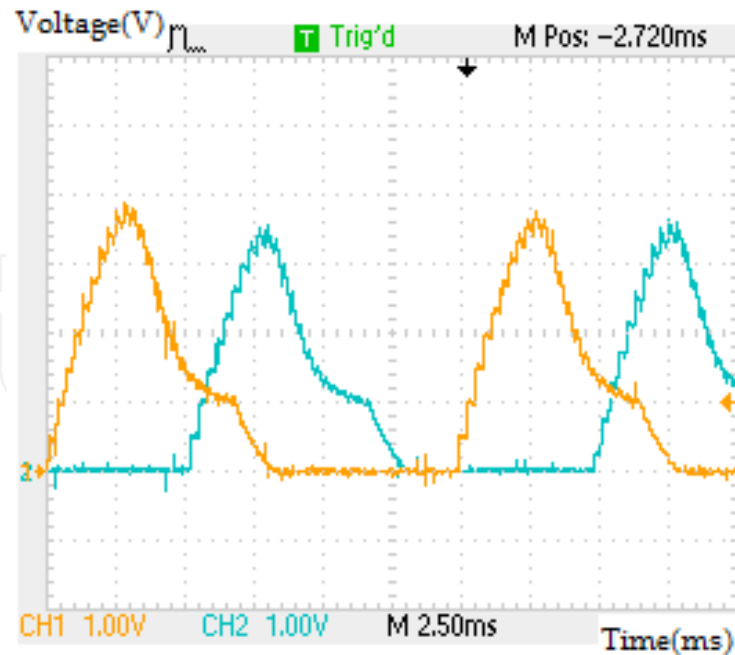 we can see that the effective current increases so as to output required torque. The out power is 3.2kW, the efficiency is 84% of the SR drive system. Figure 20 shows the two phase winding current waveform of SRM when the motor speed at 500r/min and load with peak torque.

Fig. 19. Winding current waveform of n=500r/min under loaded 72Nm

The output torque is 144N.m and output power is 6.4kw. It is obviously that winding current is controlled below the peak value (189A). The waveform of the current is flat top

and the drive system is working with full load. This status is used to provide peak torque when EV startup or accelerate. In order to improve system reliability, it is allowed to work overload for one minute. After that, the control system will lock trigger pulse and give overload alert to prevent system damage. The figure 21 shows steady state torque profile at speed of 400r/min and output power is 4kW , it shows the torque ripple is only within less than 10 N · m.
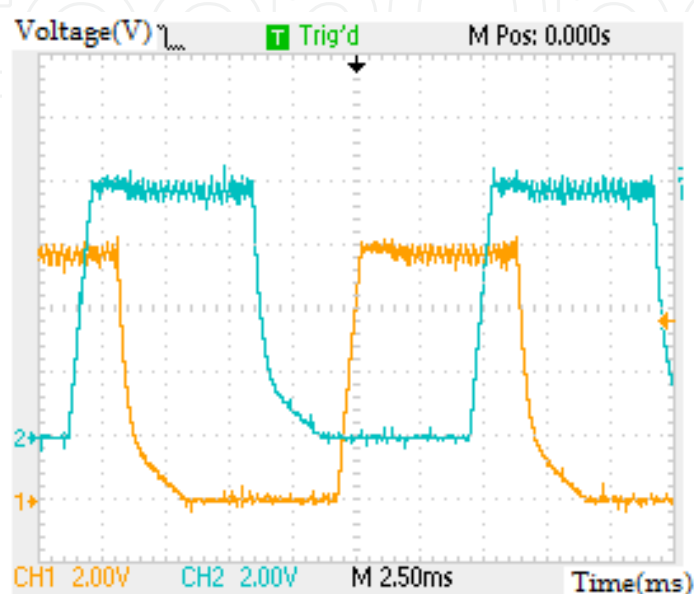
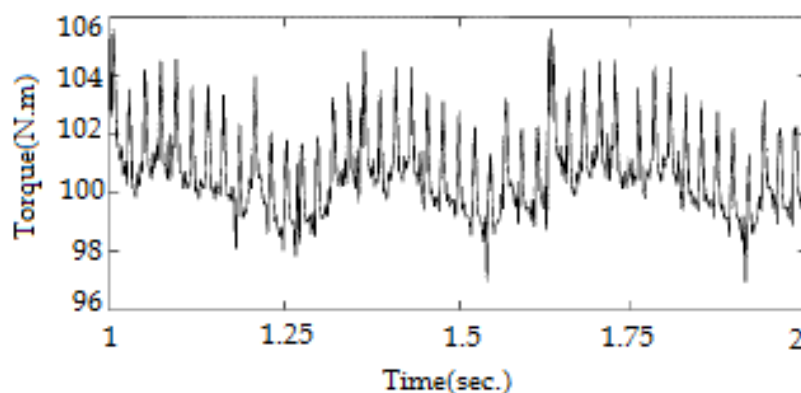Fig. 20. Winding current waveform of SRM when the motor speed at 500r/min

Fig. 21 Steady state torque profile at speed of 400r/min

5.2 Tests on the PEUGOT 505 SW8

The SR drive system designed in this chapter was installed on the PEUGEOT 505 SW8 to do vehicle tests.The van preserves clutch, gearbox and other transmission mechanism. Thus we can reduce effect on vehicle traction performance. On the other hand, in doing so can improve startup torque. The installment of Lead-acid Battery mainly considers axis

distribution and its structure. The battery is assembled by the space and axis load distribution rather than central installation to ensure the balance of front and rear bearing. The SR motor is in the position of engine and motor controller is fixed above it. It shows the excellent mechanical characteristics of the SRM when the van starts up. Pictures of the modificated EV and the SR drive system are showed respectively in figure 22 and 23. The starting torqueis almost twice the rated torque, which meet the requirement of starting, accelerating, climbing and some other complicated working conditions. The van starts up smoothly, the current of the bus is low which is less than 15A. The vehicle test was arranged with the battery which was charged full voltage (360V). The driving range was 205km. The battery voltage was 265V when the van stopped. Table 7 is running test data under different dears. Figure 24 shows the battery voltage and bus current when the EV climbed the hill which grade was greater than 25°. They were respectively 255V and 70A. The current was 120.5A when the EV accelerated and the maximum speed reached 165km/h.

Fig. 22. Modification of PEUGEOT 505 SW8

Fig. 23. SR drive system for EV

Number	Gear	Speed(r/min)	Battery voltage(V)	Bus current(A)
1	3	40	360	38
2	4	50	360	43.3
3	5	75	355	57
4	5	95	355	77
5	5	85	355	60
6	5	80	335	50
7	4	80	335	60
8	5	80	335	52
9	5	90	330	57
10	5	65	330	33
11	5	73	330	45
12	5	80	320	60
13	5	70	320	49
14	5	80	312	55
15	5	80	313	67.4
16	5	75	290	72.5
17	5	70	280	62.7

Table 7. Testing data of EV running parameter

Fig. 24 Battery voltage and bus current climbing the hill

6. Conclusion

Through the refitment of the gasoline car,the designed SR motor and drive system satisfy the demand of dynamic characteristics, the startup characteristics and the acceleration characteristics. In the stage of startup, the current of the SRM is 15A, the torque is stepless and the acceleration characteristics are quite well. The maximum speed comes up to 165kmph and the continuation of the journey reaches 205km or upward. The new rotor structure decreases the wind noise,the noise of SRM is only 76dB.

This chapter designed a 30kW SRD system used on PEUGEOT 505 SW8. The system applied fuzzy logic adaptive control based on instantaneous torque sum against the big torque fluctuation and strong noise on SRM.The vehicle tests automotive load experiment shows that the measures taken are effective. The designed SRD system has a low startup current, small torque fluctuation and high efficiency, all of which are especially suited for the dynamic characteristics of electric vehicle. So it has a broad application prospects. If the batteries and power systems are planed together, the designed SRD system will display its superiority by adjusting and integrating the subsystems.

7. Acknowledgment

8. References

J. C. Moreira, "Torque ripple minimization in switched reluctance motors via bicubic spline interpolation," *IEEE Power Electronics Specialists Conference Record*, Toledo, Spain, June 1992, 0-7803-0695-3/92, pp. 851–856.

F. Filicori, C. G. L. Bianco, and A. Tonielli, "Modeling and control strategies for a variable reluctance direct drive motor," *IEEE Trans. Industrial Electronics*, vol. 40, no. 1, pp. 105–115, 1993.

D. G. Taylor, "An experimental study on composite control of switched reluctance motors," *IEEE Control System Magazine*, vol. 11, no. 2, pp.31–36, 1991.

Nigel Schofield, Electric Vehicle Systems Notes, the University of Manchester, 2006

Yin Tianming. A novel rotor structure for SRM. China, Utility Model Matent. 03279782.6 2003

Technical information, IGBT-Module BSM300GA120DLC, EUPEC Power Electronics in Motion
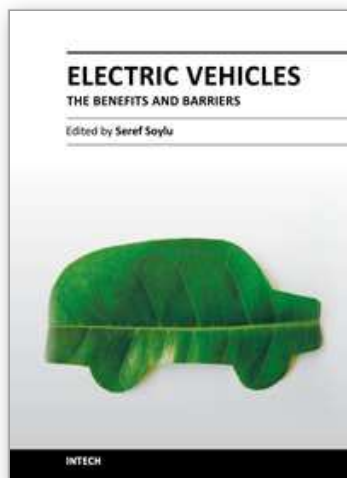
Electric Vehicles – The Benefits and Barriers

Edited by Dr. Seref Soylu

In this book, theoretical basis and design guidelines for electric vehicles have been emphasized chapter by chapter with valuable contribution of many researchers who work on both technical and regulatory sides of the field. Multidisciplinary research results from electrical engineering, chemical engineering and mechanical engineering were examined and merged together to make this book a guide for industry, academia and policy maker.

How to reference

In order to correctly reference this scholarly work, feel free to copy and paste the following:

INTECH
open science | open minds